Journal of Hazardous Materials 198 (2011) 182–187

Contents lists available at SciVerse ScienceDirect

Journal of Hazardous Materials

journal homepage: www.elsevier.com/locate/jhazmat

Size distributions and exposure concentrations of nanoparticles associated with the emissions of oil mists from fastener manufacturing processes

Ying-Fang Wang[a], Perng-Jy Tsai[a,b,*], Chun-Wan Chen[c], Da-Ren Chen[d], Yu-Tung Dai[e]

[a] Department of Environmental and Occupational Health, Medical College, National Cheng Kung University, 138, Sheng-Li Road, Tainan 70428, Taiwan
[b] Department of Occupational Safety and Health, College of Public Health, China Medical University and Hospital, 91, Hsueh-Shih Road, Taichung 40402, Taiwan
[c] Institute of Occupational Safety and Health, Council of Labor Affairs, 99, Ln. 407, Hengke Road, Xizhi City, Taipei County 22143, Taiwan
[d] Department of Energy, Environmental and Chemical Engineering, Washington University in St. Louis, One Brookings Drive, Box 1180, St. Louis, MO 63130, USA
[e] Department of Occupational Safety and Health, Chang Jung Christian University, 396, Sec. 1, Changrong Road, Guiren Dist., Tainan 71101, Taiwan

ARTICLE INFO

Article history:
Received 2 May 2011
Received in revised form 6 October 2011
Accepted 8 October 2011
Available online 15 October 2011

Keywords:
Nanoparticle
Exposure assessment
Lung deposition
Modified electrical aerosol detector
Oil mist

ABSTRACT

The aims of the present study were set out to measure size distributions and estimate workers' exposure concentrations of oil mist nanoparticles in three selected workplaces of the forming, threading, and heat treating areas in a fastener manufacturing plant by using a modified electrical aerosol detector (MEAD). The results were further compared with those simultaneously obtained from a nanoparticle surface area monitor (NSAM) and a scanning mobility particle sizer (SMPS) for the validation purpose. Results show that oil mist nanoparticles in the three selected process areas were formed mainly through the evaporation and condensation processes. The measured size distributions of nanoparticles were consistently in the form of uni-modal. The estimated fraction of nanoparticles deposited on the alveolar (AV) region was consistently much higher than that on the head airway (HD) and tracheobronchial (TB) regions in both number and surface area concentration bases. However, a significant difference was found in the estimated fraction of nanoparticles deposited on each individual region while different exposure metrics were used. Comparable results were found between results obtained from both NSAM and MEAD. After normalization, no significant difference can be found between the results obtained from SMPS and MEAD. It is concluded that the obtained MEAD results are suitable for assessing oil mist nanoparticle exposures.

1. Introduction

The manufacture of fasteners involves seven industrial processes, including the wiredrawing, forming, threading, cleaning, heat treatment, surface treatment, and packaging and shipping. Among them, the mineral oil-based metalworking fluids (MWFs) are used in forming, threading, and heat treatment processes, and thus might result in the emissions of oil mists to the workplace atmosphere and cause workers' exposures [1,2]. Epidemiological and animal studies have indicated that oil mist exposures might result in the laryngeal cancer, asthma, bronchial hyperresponsiveness, lipoid pneumonia, and lung cancer [3–6].

In principle, machining operations would mainly generate aerosols with particle sizes greater than 1 μm. However, the emissions of sub-micron and nano-sized particles could still be possible [7–10]. Heitbrink et al. have reported that aerosols generated from an engine machining and assembly facility fell to the range from 0.023 μm to 0.1 μm [11]. In particular, for those involve 'hot' processes, such as welding, heat treatment, and high-speed machining processes, are known to generate nanoparticles [1,12–14]. It is known that MWFs are semi-volatile in nature, nanoparticles could be formed by the evaporation and condensation mechanisms after MWFs being "heated" during manufacturing processes [15,16]. However, it should be noted that very few studies have been conducted to address workers' exposures to nanoparticles arising from MWF emissions in workplaces.

Nanoparticles are known for particles with diameters less than 0.1 μm (or 100 nm) [17]. Nanoparticles might cause serious inflammation in the deep lung because of their large particle numbers and surface areas [18–20]. Recent toxicological studies have suggested that they can easily penetrate cells or tissues and result in many irreversible pulmonary health effects [21–23]. It has also been found that nanoparticles can penetrate to the brain via nasal mucosa and olfactory buds [23]. It is known that both surface area and number concentrations are better exposure metrics for assessing adverse health effects caused by nanoparticle exposures than the mass concentration [24–28]. In addition, adverse health effects associated with nanoparticle exposures are also affected by their

* Corresponding author at: Department of Environmental and Occupational Health, Medical College, National Cheng Kung University, 138, Sheng-Li Road, Tainan 70428, Taiwan. Tel.: +886 6 2353535x5806; fax: +886 6 2752484.
E-mail address: pjtsai@mail.ncku.edu.tw (P.-J. Tsai).

0304-3894/$ – see front matter © 2011 Elsevier B.V. All rights reserved.
doi:10.1016/j.jhazmat.2011.10.028

deposited regions in the respiratory tract. Therefore, simultaneously estimating both the surface area and number concentrations of nanoparticles exposed to different regions of the respiratory tract is considered a better approach for characterizing nanoparticle exposures.

Many instruments, such as the condensation particle counter (CPC; Model 3020, TSI Inc., Shoreview, MN, USA), scanning mobility particle sizer (SMPS; Model 3934, TSI Inc., Shoreview, MN, USA), electrical low-pressure impactor (ELPI; Dekati Ltd., Tampere, Finland), and nano-micro-orifice uniform deposit impactor (Nano-MOUDI; Model 110, MSP Corp., Shoreview, MN, USA), have been used in the field for providing data to predict nanoparticle exposures to workers of various industries. However, the aforementioned devices cannot be directly used to estimate the surface area nanoparticle concentrations deposited in different regions of the respiratory tract. Recently, a nanoparticle surface area monitor (NSAM; Model 3550, TSI Inc., Shoreview, MN, USA) has been developed, based on the particle charging characteristics of an electrical aerosol detector (EAD; Model 3070a, TSI Inc., Shoreview, MN, USA), to directly estimate surface area concentrations of nanoparticles deposited on both TB and AV regions of the respiratory tract [29,30]. However, it should be noted that the above instrument can neither simultaneously estimate the surface area concentration of the HD region, nor the number concentrations of the HD, TB, and AV regions. More recently, a modified EAD (MEAD) has been developed by our research group to overcome the above mentioned shortcomings [31,32], and the device had been successfully used in the carbon black manufacturing workplaces [33].

The purposes of the present study were set out to use the MEAD to characterize size distributions of oil mist nanoparticles and estimate their exposure concentrations to different regions of the respiratory tract. Considering both surface area and number concentrations are better exposure metrics than the mass concentration for assessing adverse health effects caused by nanoparticle exposures [24–28], only the first two metrics were used to assess fastener manufacturing workers exposures in the present study. For the validation purpose, the measured surface area and number concentrations were further compared with those simultaneously obtained from SMPS and NSAM.

2. Materials and methods

2.1. Sampling sites

Field samplings were conducted at the three manufacturing processes of the forming, threading, and heat treatment associated with the use of MWFs. For the former two processes, they might result in the increase in wire temperatures since both impaction and compression processes were involved. As a result, MWFs are used for the purpose of reducing the wire temperature and extending machine life. After the threading process, the treaded products are quenched by passing through MWFs. Then, the products are annealed to room temperature. Finally, they are tempered by raising temperatures from 650 °C to 1500 °C to obtain products with requested hardness and toughness [34].

In the present study, an outdoor sampling site, located at the outside of office building of the selected fastener manufacturing plant, was also selected to determine the background nanoparticle concentration.

2.2. Sampling instruments

A MEAD was used to conduct samplings for nanoparticles in the present study. The MEAD was installed with a high voltage power supply (Stanford Research Systems Inc., Model PS325/2500 V–25 W, Sunnyvale, CA, USA) to have its voltages of the ion trap become variable (range: 20–2500 V). During samplings, the readings of the electrometer were recorded while the voltages of the ion trap were consecutively set at 20 V, 100 V, 200 V, 500 V, 1000 V, 1500 V, 2000 V, and 2500 V (each for 10 s), respectively, for each run [31]. Two reference instruments were simultaneously used to measure nanoparticles in order to validate results obtained from the MEAD. The first one was the NSAM (TSI Inc., Model 3550, St. Paul, MN, USA) which was used to estimate surface area concentrations of nanoparticles deposited on both TB and AV regions of the respiratory tract [30]. The detectable particle size range for the NSAM is 10–1000 nm and surface area concentration range for TB and AV regions are 0–2500 $\mu m^2\ cm^{-3}$ and 0–10,000 $\mu m^2\ cm^{-3}$, respectively. The second one was the SMPS (TSI Inc., Model 3936, St. Paul, MN, USA) which was used to measure the number concentrations of nanoparticles of different particle sizes. The detectable particle size range for the SMPS is 14.1–737 nm and maximum particle concentration is 10^7 particles cm^{-3}.

2.3. Sampling methods

For all selected workplaces (including the forming, threading, heat treatment processes, and outdoor sampling site), samplings were conducted for continuous four days. On each sampling day for each selected workplace, one MEAD, one NSAM and one SMPS were placed side-by-side at the location nearest to worker's breathing zone (i.e., location ~1.5 m above the ground level). Samplings were conducted from 08:00 AM to 10:00 AM and from 08:00 AM to 12:00 AM to determine the outdoor atmospheric background concentration and workers' daily exposure concentrations, respectively. Considering production activity in these three selected areas was constant (i.e., contains three eight hour workshifts), no workplace background concentrations could be measured.

2.4. Data analyses

In the present study, a data-reduction scheme was used to retrieve the size distribution of sampled nanoparticles based on readings obtained the eight preset voltages of the MEAD. Detailed computation processes can be seen in our previous publication [31]. The resultant size distributions were used to predict depositions of nanoparticles at the HD, TB, and AV regions of the respiratory tract using the UK National Radiological Protection Board's (NRPB's) LUDEP Software [35]. The above software was established based on ICRP 66 lung deposition models [36]. In the present study, we assumed the breathing pattern of workers can be described as follows:

- Breathing type: nose only
- Functional lung residual capacity: 3301 mL
- Breathing rate: 20 breath/min
- Ventilation rate: 1.5 m^3/h
- Activity level: light exercise.

The above criteria were the same as that prescribed for NSAM [30]. Fig. 1 shows three predicted deposition curves of the HD, TB, and AV regions based on the above assumptions, respectively. Here, it should be noted that the above predicted deposition curves are only suitable for workers under the light exercise with the nose-only breathing condition. The above working scenario was quite comparable to those workers in the three selected processes via our field observations.

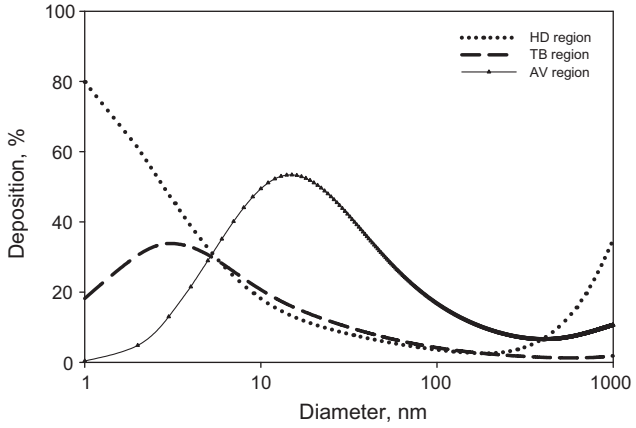

Fig. 1. Calculated particle deposition curves as a function of particle size for the Head Airway (HD), Tracheobronchial (TB), and Alveolar (AV) regions of a human lung (based on the model given in ICRP [36]).

Table 1
Number-based size distributions of nanoparticles (1–1000 nm) measured by the MEAD in the three selected workplaces and background ambient environment ($n = 6$).

Work area	Number-based size distribution (nm)	
	CMD (range)	σ_g
Forming	26.9 (25.3–30.1)	2.64
Threading	23.2 (21.1–25.2)	2.86
Heat treating	22.5 (20.3–25.2)	2.98
Ambient[a]	41.1	2.21

[a] $n = 1$.

3. Results and discussion

3.1. Size distributions of nanoparticles

Table 1 shows size distributions of nanoparticles (measured particle size range: 1–1000 nm) in the atmosphere of the three selected workplaces and the outdoor ambient air. It can be seen that the count median diameter (CMD) and the corresponding geometric standard deviation (σ_g) for nanoparticles of the outdoor ambient air were 41.1 nm and 2.2, respectively. The above results were similar to the results obtained from Heitbrink et al. [11] and Wake [37]. As shown in Fig. 2, size distributions of nanoparticles were consistently in the form of the uni-modal for samples collected from the forming area, threading area, and heat treating area with CMD and its corresponding σ_g as 26.9 nm and 2.64, 23.2 nm and 2.86, and 22.5 nm and 2.98, respectively. The above results were similar to the results obtained from SMPS measurements (the forming area, threading area, and heat treating area with CMD and its corresponding σ_g as 28.6 nm and 2.54, 24.3 nm and 2.77, and 21.9 nm and 2.62, respectively). In an engine machining and assembly facility workplace atmosphere, Heitbrink et al. found that the resultant uni-modal nanoparticles could be mainly contributed by the evaporation/condensation because of MWFs being heated at the interface between the tools and the components during the machine operations [11]. At this stage, it might not be possible to explain the intrinsic differences in CMD among three studied industrial processes because factors associated with the evolution of aerosols in the field were very complicated (such as saturated vapor pressure, surface tension, and molecular weights of the involved MWFs, etc.) [38,39]. However, our results are quite comparable to those conducted by Heitbrink et al. (i.e., particle size range = 20–40 nm) [11].

3.2. Number concentrations and surface area concentrations of nanoparticles

Table 2 shows the number and surface area concentrations of nanoparticles for the outdoor atmospheric background and the three selected workplaces. The mean number concentrations for the forming area, threading area, and heat treating area (=1.42–3.47 $\times 10^5$ particles cm^{-3}) were significantly higher than that of the outdoor environment (=0.126 $\times 10^5$ particles cm^{-3}) ($p < 0.05$). The above results clearly indicate that process emissions could effectively elevate the number concentrations of nanoparticles in workplace atmospheres. However, we also found that their workplace concentrations fell within the range obtained from an engine machining and assembly plant (=0.29–4.4 $\times 10^5$ particles cm^{-3}) [11].

The mean number concentrations obtained from the forming area (=2.13 $\times 10^5$ particles cm^{-3}) were significantly higher than the threading area (=1.42 $\times 10^5$ particles cm^{-3}) (nonparametric Mann–Whitney test, $p < 0.05$). Based on our previous study [38], the measured surface temperatures on the molder of the forming machine (=75.8 ± 19.8 °C) were higher than that on the surface of the threading gear (=69.6 ± 17.1 °C). In addition, we also found that the workplace area of the threading process (=734.4 m^2) was much larger than that of forming process (=194.7 m^2). Therefore, it could be expected that the forming area had higher number concentrations than that of the threading area by considering the generation of oil mists due to the evaporation and condensation processes, and the dilution effect associated the volumes of the above two workplaces. Finally, we found the heat treating area had the highest number concentration among the three selected industrial processes ($p < 0.005$). In the present study, the temperatures measured from those MWFs tanks used in quenching and tempering steps of heat treating operations (850–1300 °C and 650–1300 °C, respectively) were much higher than the temperatures measured from the other two processes (as described above). Indeed, both temperatures of fluid and air would affect how semi-volatile substances can evaporate and condensate in the workplace atmosphere [40,41]. Since the workplace temperatures of the heat treating process were still less than 30 °C, the highest number concentration found in the heat treating process would be theoretically plausible.

Finally, the trends found in the number concentrations (as described above) can also be seen in their corresponding surface area concentrations. In the present study, significant

Table 2
Estimated total number concentrations (10^5 particles cm^{-3}) and total surface area concentrations (10^3 μm^2 cm^{-3}) for nanoparticles (1–1000 nm) found in the three selected workplaces and background ambient environment ($n = 6$).

Work area	Total number concentration (10^5 particles cm^{-3})		Total surface area concentration (10^3 μm^2 cm^{-3})	
	Mean ± SD	Range	Mean ± SD	Range
Forming	2.13 ± 1.05	1.23–3.35	3.06 ± 1.14	1.77–4.82
Threading	1.42 ± 0.572	0.772–2.33	2.03 ± 0.733	1.11–3.33
Heat treating	3.47 ± 1.22	2.05–4.80	5.39 ± 1.46	3.18–7.48
Ambient[a]	0.126	–	0.218	–

[a] $n = 1$.

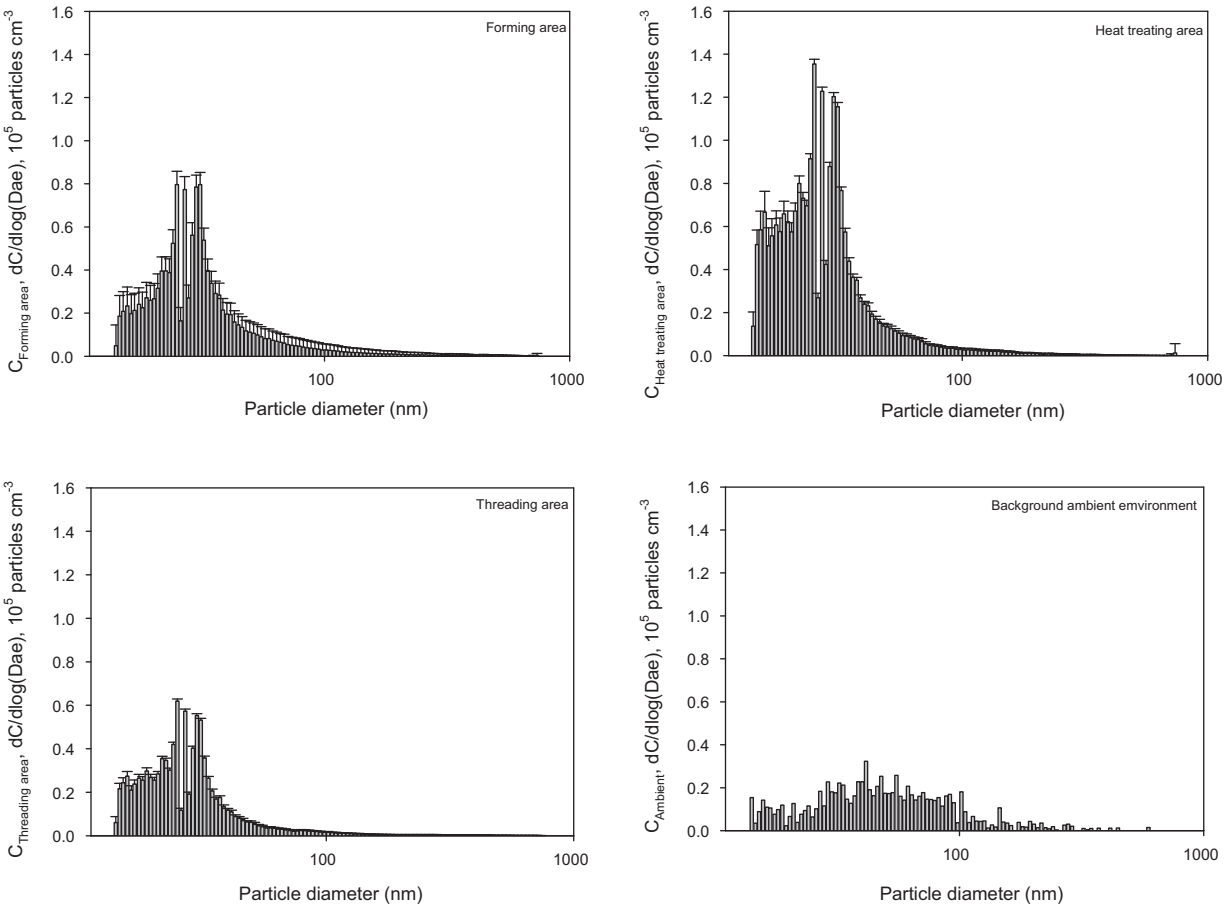

Fig. 2. Particle number-based size distributions estimated by using the MEAD in the three selected workplaces and the background ambient environment.

differences can be found between the mean surface area concentration of the outdoor atmospheric background (=0.218×10^3 $\mu m^2\ cm^{-3}$) and that of the three selected areas (=$1.11–7.48 \times 10^3$ $\mu m^2\ cm^{-3}$) ($p < 0.05$). Moreover, workplace concentrations of the threading area (=2.03×10^3 $\mu m^2\ cm^{-3}$) and the forming area (=3.06×10^3 $\mu m^2\ cm^{-3}$) were lower than that of the heat treating area (=5.39×10^3 $\mu m^2\ cm^{-3}$).

Furthermore, we compared the estimated number concentrations of the three workplaces obtained from MEAD with that obtained from SMPS. Significant differences can be found between values (paired *t*-test, $p < 0.05$) obtained from MEAD and that from SMPS. In particular, values obtained from the MEAD were consistently higher than that from SMPS (Fig. 3a). Considering measuring principles of the MEAD were different from those of SMPS, the existence of systemic differences between their measured results could be theoretically plausible. A similar result can also be found in a study conducted by Woo et al. in measuring atmospheric nanoparticle concentrations [42]. In this study, the measured number concentrations obtained from the SMPS were used as the reference to normalize the corresponding values obtained from the MEAD. No significant difference can be found between the measured values obtained from SMPS and the corresponding normalized MEAD values (paired *t*-test, $p > 0.05$) (Fig. 3b). The relationship between the results obtained from SMPS (i.e., x) and the normalized MEAD results (i.e., y) was found as $y = 0.93\ x$ ($n = 18$, corrected-$R^2 = 0.74$). Therefore, the number concentrations obtained from MEAD could be further validated.

3.3. Estimated concentrations of nanoparticles deposited on different regions of the respiratory tract

In this study, the measured size distribution data was further used to estimate both the number and surface area concentrations of nanoparticles deposited on different regions of the respiratory tract for the three selected workplaces. Table 3 shows the estimated number concentration results. Obviously, it can be seen that the estimated number concentrations (and fractions) of nanoparticles deposited on the three regions shared the same trend for three selected workplaces as: AV > TB > HD. In particular, the fraction of nanoparticles deposited on the AV region was much higher

Table 3
Estimated number concentrations (10^5 particles cm^{-3}) deposited in the HD, TB, and AV regions of the respiratory tract for nanoparticles (1–1000 nm) found in the three selected workplaces ($n = 6$).

Work area	Total deposited conc.	HD		TB		AV	
		Conc.	Fraction (%)	Conc.	Fraction (%)	Conc.	Fraction (%)
Forming	1.38 ± 1.07	0.252 ± 0.203	18	0.275 ± 0.221	20	0.861 ± 0.643	62
Threading	0.922 ± 0.372	0.191 ± 0.083	21	0.204 ± 0.082	22	0.536 ± 0.212	57
Heat treating	2.27 ± 0.791	0.515 ± 0.176	22	0.517 ± 0.183	22	1.27 ± 0.454	56

Table 4
Estimated surface area concentrations (10^2 μm^2 cm^{-3}) deposited in the HD, TB, and AV regions of the respiratory tract for nanoparticles (1–1000 nm) found in the three selected workplaces (n = 6).

Work area	Total deposited conc.	HD		TB		AV	
		Conc.	Fraction (%)	Conc.	Fraction (%)	Conc.	Fraction (%)
Forming	11.1 ± 5.90	2.73 ± 1.45	25	1.64 ± 0.873	15	6.71 ± 3.57	60
Threading	4.97 ± 2.01	1.37 ± 0.551	28	0.705 ± 0.298	14	2.89 ± 1.17	58
Heat treating	13.2 ± 4.57	3.91 ± 1.37	30	1.77 ± 0.627	14	7.34 ± 2.57	56

than that of the other two regions for all selected workplaces. Table 4 shows the results associated with the estimated surface area concentration. It can be seen that the estimated surface area concentrations also shared the same trend for three selected workplaces as: AV > HD > TB. Again, the fraction of nanoparticles deposited on the AV region was also much higher than that of the other two regions for all selected workplaces. However, by comparing the results shown in Tables 3 and 4, significant differences can be found in the fractions of nanoparticles deposited on each individual region while different exposure metrics were adopted. Our results clearly indicate the importance for simultaneously measuring both the surface area and number concentrations of nanoparticles deposited on different regions of the respiratory tract for nanoparticle exposure assessments.

Fig. 4 compares the results of the surface area concentrations deposited on both the TB and the AV regions obtained from MEAD with that obtained from NSAM. For the concentrations estimated for the TB region, the results obtained from the NSAM for the forming area, threading area, and heat treating area quite comparable to those corresponding values obtained from MEAD (t-test, $p > 0.05$). The same trend can also be found for the concentrations estimated for the AV region (t-test, $p > 0.05$). Considering both NSAM and MEAD sharing the same measuring principles (i.e., particle charging efficiency and particle electrical mobility), comparable results obtained from both instruments could be theoretically expectable.

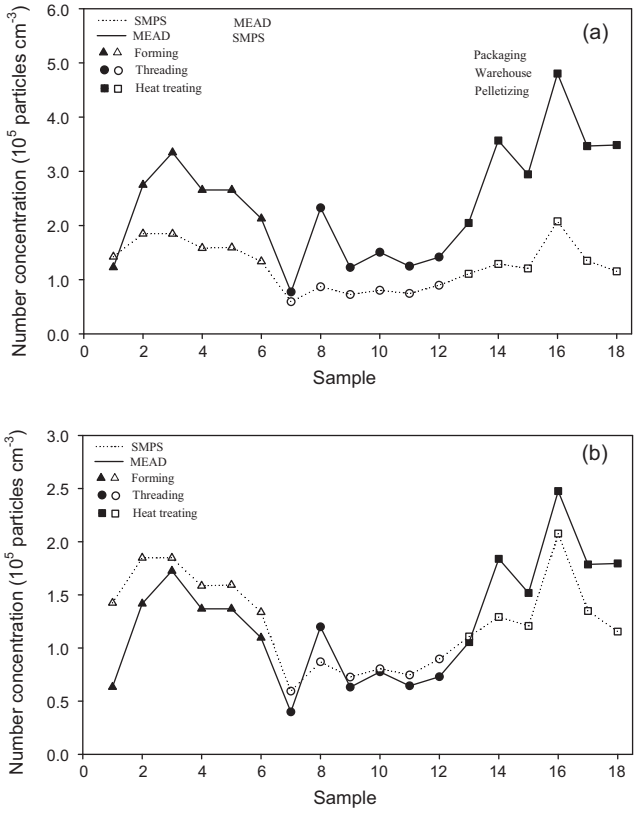

Fig. 3. Comparing number concentrations obtained from SMPS with that from MEAD: (a) non-normalized; (b) after being normalized.

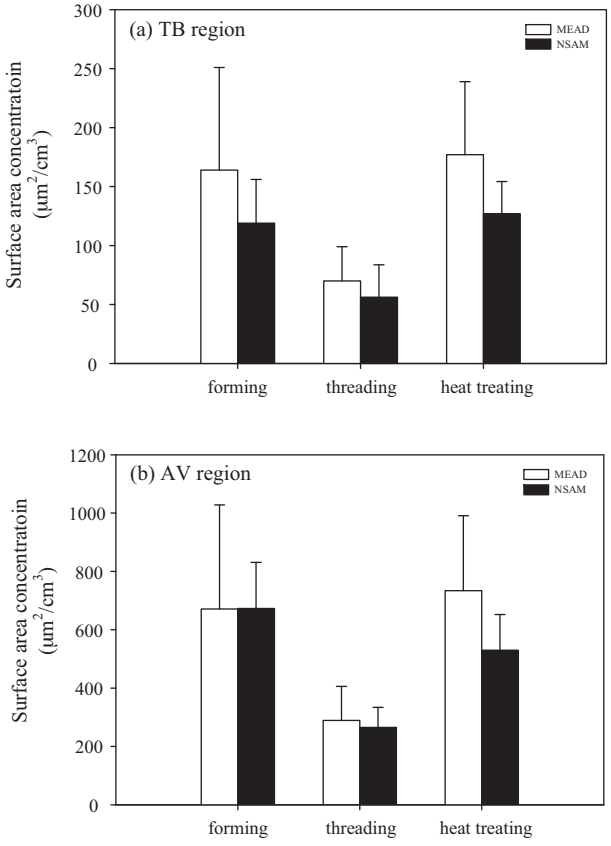

Fig. 4. Confirmations of nanoparticles deposited on (a) TB region and (b) AV region for samples collected by the MEAD and NSAM.

4. Conclusions

We found that size distributions of nanoparticles were consistently in the form of uni-modal for the three selected process areas. It could be mainly explained by the evaporation and condensation processes of MWFs. For both number and surface area concentrations, the fractions of nanoparticles deposited on the AV region were much higher than that of the other two regions of the TB and HD for all selected workplaces. However, a significant difference was found in the fractions of nanoparticles deposited on each individual region of the respiratory tract while different exposure metrics were adopted. Our results clearly indicate the importance for simultaneously measuring both the surface area and number concentrations of nanoparticles deposited on different regions of the respiratory tract for nanoparticle exposure assessments. In the present study, results obtained from both NSAM and MEAD were quite comparable. In addition, no significant difference could be found between the measured values obtained from SMPS and the

corresponding MEAD values after being normalized. The above results clearly indicate that the measured MEAD results would be theoretically plausible.

Acknowledgements

We are grateful to the Institute of Occupational Safety and Health (IOSH) in Taiwan for funding this research project. One of the co-authors, Y.-T. Dai, has the same contribution as the corresponding author in this research work.

References

[1] D.L. Thornburg, Mist generation during metal machining, J. Tribol. 122 (2000) 544–549.
[2] D.J. Michalek, W.W.S. Hii, J.S. Sun, K.L. Gunter, Experimental and analytical efforts to characterize cutting fluid mist formation and behavior in machining, Appl. Occup. Environ. Hyg. 18 (2003) 842–854.
[3] M. Russi, R. Dubrow, J.T. Flannery, M.R. Cullen, S.T. Mayne, Occupational exposure to machining fluids and laryngeal cancer risk: contrasting results using two separate control groups, Am. J. Ind. Med. 31 (1997) 166–171.
[4] A.E. Ellen, J.S. Thomas, K. David, R.W. Susan, J.M. Douglas, M.K. Susan, S. Stuart, R.M. Richard, Respiratory health of automobile workers and exposures to metal-working fluid aerosols: lung spirometry, Am. J. Ind. Med. 39 (2001) 443–453.
[5] S.M. Kennedy, Y.M. Chan, K. Teschke, B. Karlen, Change in airway responsiveness among apprentices exposed to metalworking fluids, Am. J. Respir. Crit. Care Med. 159 (1999) 87–93.
[6] N. Kazerouni, T.L. Thomas, S.A. Petralia, R.B. Hayes, Mortality among workers exposed to cutting oil mist: update of previous reports, Am. J. Ind. Med. 38 (2000) 410–416.
[7] T.L. Chan, J.B. D'Arcy, J. Siak, Size characteristics of machining fluid aerosols in an industrial metalworking environment, Appl. Occup. Environ. Hyg. 5 (1990) 162–170.
[8] J. Dash, J.B. D'Arcy, A. Gundrum, J. Sutherland, J. Johnson, D. Carlson, Characterization of fine particles from machining in automotive plants, J. Occup. Environ. Hyg. 2 (2005) 609–625.
[9] W.A. Heitbrink, J.B. D'Arcy, J.M. Yacher, Mist generation at a machining center, Am. Ind. Hyg. Assoc. J. 61 (2000) 22–30.
[10] W.A. Heitbrink, J.M. Yacher, G.J. Deye, A.B. Spencer, Mist control at machining center. Part 1: mist characterization, Am. Ind. Hyg. Assoc. J. 61 (2000) 275–281.
[11] W.A. Heitbrink, D.E. Evans, T.M. Peters, T.J. Slavin, Characterization and mapping of very fine particles in an engine machining and assembly facility, J. Occup. Environ. Hyg. 4 (2007) 341–351.
[12] J. Vincent, C. Clement, Ultrafine particles in workplace atmospheres, Philos. Trans.: Math. Phys. Eng. Sci. 358 (2000) 2673–2682.
[13] A.S. Ross, K. Teschke, M. Brauer, S.M. Kennedy, Determinants of exposure to metalworking fluid aerosol in small machine shops, Ann. Occup. Hyg. 48 (2004) 383–391.
[14] J.R. Portela, J. Lopez, E. Nebot, E. Martínez de la Ossa, Elimination of cutting oil wastes by promoted hydrothermal oxidation, J. Hazard. Mater. 88 (2001) 95–106.
[15] J. Thornburg, D. Leith, Size distribution of mist generated during metal machining, Appl. Occup. Environ. Hyg. 15 (2000) 618–628.
[16] J.F. Pankow, An absorption model of the gas/particle partitioning of organic compounds in the atmosphere, Atmos. Environ. 28 (1994) 185–188.
[17] A. Peters, H.E. Wichmann, T. Tuch, J. Heinrich, J. Heyder, Respiratory effects are associated with the number of ultrafine particles, Am. J. Respir. Crit. Care Med. 155 (1997) 1376–1383.
[18] W.G. Kreyling, M. Semmler, F. Erbe, P. Mayer, S. Takenaka, H. Schulz, Translocation of ultrafine insoluble iridium particles from lung epithelium to extrapulmonary organs is size dependent but very low, J. Toxicol. Environ. Health 65 (2002) 1513–1530.
[19] G. Oberdörster, Pulmonary effects of inhaled ultrafine particles, Int. Arch. Occup. Environ. Health 74 (2001) 1–8.
[20] K. Donaldson, D. Brown, A. Clouter, R. Duffin, W. MacNee, L. Renwick, L. Tran, V. Stone, The pulmonary toxicology of ultrafine particles, J. Aerosol Med. 15 (2002) 213–220.
[21] D.W. Dockery, C.A. Pope, X. Xu, J.D. Spengler, J.H. Ware, M.E. Fay, An Association between air pollution and mortality in six U.S. cities, N. Engl. J. Med. 329 (1993) 1753–1759.
[22] G. Oberdörster, Toxicology of ultrafine particles: in vivo studies, Philos. Trans. R. Soc. Lond. A 358 (2000) 2719–2740.
[23] E. Oberdörster, Manufactured nanomaterials (Fullerenes C60) induce oxidative stress in the brain of juvenile largemouth bass, Environ. Health Perspect. 112 (2004) 1058–1062.
[24] G. Oberdörster, Significance of particle parameters in the evaluation of exposure–dose–response relationships of inhaled particles, Part. Sci. Technol. 14 (1996) 135–151.
[25] K. Donaldson, X.Y. Li, W. MacNee, Ultrafine (nanometer) particle mediated lung injury, J. Aerosol Sci. 29 (1998) 553–560.
[26] C.L. Tran, D. Buchanan, R.T. Cullen, A. Searl, A.D. Jones, K. Donaldson, Inhalation of poorly soluble particles. Influence of particle surface area on inflammation and clearance, Inhal. Toxicol. 12 (2005) 1113–1126.
[27] A. Elder, R. Gelein, J.N. Finkelstein, K.E. Driscoll, J. Harkema, G. Oberdörster, Effects of subchronically inhaled carbon black in three species. Retention kinetics, lung inflammation, and histopathology, Toxicol. Sci. 88 (2005) 614–629.
[28] T. Stoeger, C. Reinhard, S. Takenaka, A. Schroeppel, E. Karg, B. Ritter, J. Heyder, H. Schulz, Instillation of six different ultrafine carbon particles indicates a surface area threshold dose for acute lung inflammation in mice, Environ. Health Perspect. 114 (2006) 328–333.
[29] W.E. Wilson, H.S. Han, J. Stanek, J. Turner, D.R. Chen, D.Y.H. Pui, Use of the electrical aerosol detector as an indicator of the surface area of fine particles deposited in the lung, J. Air Waste Manage. Assoc. 57 (2007) 211–220.
[30] H. Fissan, A. Trampe, S. Neunman, D.Y.H. Pui, W.G. Shin, Rationale and principle of an instrument measuring lung deposition area, J. Nanopart. Res. 9 (2007) 53–59.
[31] L. Li, D.R. Chen, P.J. Tsai, Use of an electrical aerosol detector (EAD) for nanoparticle size distribution measurement, J. Nanopart. Res. 11 (2009) 111–120.
[32] L. Li, D.R. Chen, P.J. Tsai, Evaluation of an electrical aerosol detector (EAD) for the aerosol integral parameter measurement, J. Electrostat. 67 (2009) 765–773.
[33] Y.F. Wang, P.J. Tsai, C.W. Chen, D.R. Chen, D.J. Hsu, Using a modified electrical aerosol detector (MEAD) to predict nanoparticle exposures to different regions of the respiratory tract for workers in a carbon black manufacturing industry, Environ. Sci. Technol. 44 (2010) 6767–6774.
[34] H.H. Daniel, D.S. Richard, Heat treating fasteners – Part 1: Tips of the trade, Fastener Technol. Int. (2008) 34–37.
[35] A.C. James, M.R. Bailey, M.D. Dorrian, LUDEP Software, Version 2.07: Program for Implementing ICRP 66 Respiratory Tract Model. RPB, Chilton, Didcot, OXON. OX11 ORQ UK, 2000.
[36] ICRP, International Commission on Radiological Protection, Human Respiratory Tract Model for Radiological Protection, Publication 66, Oxford, Pergamon, London, UK, 1994.
[37] D. Wake, Ultrafine particles in the workplace, HSL Report number ECO/00/18, 2001.
[38] M.R. Chen, P.J. Tsai, C.C. Chang, T.S. Shih, W.J. Lee, P.C. Liao, Particle size distributions of oil mists in workplace atmospheres and their exposure concentrations to workers in a fastener manufacturing industry, J. Hazard. Mater. 146 (2007) 393–398.
[39] W.C. Hinds, Condensation and evaporation, in: Aerosol Technology Properties, Behavior and Measurement of Airborne Particles, 2nd ed., John Wiley and Sons, Inc., New York, USA, 1999, pp. 278–303.
[40] S. Cooper, D. Leith, Evaporation of metalworking fluid mist in laboratory and industrial mist collectors, AIHA J. 59 (1998) 45–51.
[41] R.C Raynor, S. Cooper, D. Leith, Evaporation of polydisperse multicomponent oil droplets, AIHA J. 57 (1996) 1128–1136.
[42] K.S. Woo, D.R. Chen, D.Y.H. Pui, W.E. Wilson, Use of continuous measurements of integral aerosol parameters to estimate particle surface area, Adsorpt. Sci. Technol. 34 (2001) 57–65.